Measurement of activation energies for field evaporation of tungsten ions as a function of electric field

G. L. Kellogg
Sandia National Laboratories, Albuquerque, New Mexico 87185
(Received 26 September 1983)

Activation energies for the field evaporation of tungsten ions have been determined as a function of electric field in the range from 4.70 to 5.90 V/Å. Field-evaporation rates covering 2—3 orders of magnitude were measured as a function of temperature at seven different field strengths with the use of calibrated imaging atom-probe mass spectra, and the activation energies and frequency prefactors were obtained from standard Arrhenius plots. The activation energies were found to decrease from 0.89 ± 0.05 to 0.12 ± 0.03 eV as the electric field was increased from 4.70 to 5.90 V/Å. These experimental results strongly disagree with calculations based on the image-force model of field evaporation, and a correction to the model involving field-induced charge transfer is suggested. As expected, the activation energies for field evaporation of W^{3+} and W^{4+} were found to be the same and give support for recent post-ionization models. Contrary to expectations, the frequency prefactor, which had been assumed to be constant, was found to be field dependent. This report also includes new measurements of the temperature dependence of the W evaporation field and the field dependence of the W evaporation rate. Measurements of the field-evaporation activation energy in background pressures above 5×10^{-10} Torr indicate that very low levels of contamination can reduce the activation energy by more than a factor of 4.

I. INTRODUCTION

Field evaporation is the removal of atoms from a solid surface by a high electric field.[1] A potentially important application of the field-evaporation process is the direct determination of the binding strengths of surface atoms from the electric field required for their removal. Since field evaporation is typically carried out on samples whose surface can be imaged in atomic detail with the field-ion microscope,[1] it should be possible to obtain these binding strengths specific to a particular atomic site. Unfortunately, past attempts to obtain binding energies of surface atoms from field-evaporation measurements[2,3] have been considered invalid because existing field-evaporation models do not properly account for the polarization of the surface atoms by the high electric field.[4] In order to obtain reliable data on binding energies, the polarization contribution must be determined. This in turn requires extensive experimental data on well-defined surfaces.

Although low-temperature evaporation fields have been determined for a number of elements,[1] systematic data on the variation of field-evaporation parameters with field and temperature are scarce. Tsong's[5] measurements of the variation in the tungsten field-evaporation rate with applied electric field have provided the most sensitive test of existing field-evaporation theories and have been used to calculate the polarizability of kink-site and adatom-site surface atoms. The parameters he obtained, however, turned out to be dependent on the model chosen, and other investigators have given different interpretations of the experimental data.[6] An equally important test of existing field-evaporation models is the variation in field-evaporation rate with temperature, from which the activation energy for field evaporation can be calculated. This type of measurement has recently been reported by Ernst[7] for rhodium samples. Ion counting rates were measured as a function of increasing temperature over a field range from 1.7—4.1 V/Å in a magnetic sector, field-desorption mass spectrometer. Because dc field evaporation was employed, the variation in the rate of evaporation at a given field was restricted to approximately 1 order of magnitude corresponding to temperature changes of ~50 K.

In this paper we report measurements of the tungsten field-evaporation rate as a function of temperature using pulsed field evaporation. At a given field strength, the temperature was varied by 120—180 K, which produced changes in the field-evaporation rate of 2—3 orders of magnitude. The activation energy of field evaporation and the Arrhenius prefactor were determined from these measurements at seven different electric field strengths. The results are discussed in relation to existing field-evaporation theories and the polarization of surface atoms. This paper also includes (1) a comparison between the activation energy of field evaporation for W^{4+} and W^{3+}, (2) new data on the change in field-evaporation rate with electric field, (3) measurements of the reduction in evaporation field with increasing temperature, and (4) data indicating a strong influence of surface contamination in activation energy measurements. The data presented here are intended to stimulate new theoretical models which properly account for high-field polarization and ultimately lead to the possibility of using field evaporation to extract the binding energies of individual surface atoms.

II. FIELD-EVAPORATION THEORY

Provided that field evaporation takes place above temperatures where ionic tunneling occurs (calculated in Ref.

2 to be ~ 40 K), the rate of field evaporation, k, is given by an Arrhenius rate equation of the form[8]

$$k = k_0 e^{-Q(F)/k_B T}, \tag{1}$$

where k_0 is a frequency factor, $Q(F)$ is the field-dependent activation energy of field evaporation, k_B is a Boltzmann's constant, and T is the temperature. Two different analytical expressions have been derived for the activation energy of field evaporation based on two different physical models. In the "image-force" model,[9] field evaporation is considered to be an activation of an ion with charge n over a potential barrier formed by the superposition of the field potential $-neFx$, and the image potential of the ion $-n^3e^2/4x$. According to this model, the activation energy of field evaporation is given by

$$Q(F) = \Lambda + \sum_n I_n - n\phi - (n^3e^3F)^{1/2} + \tfrac{1}{2}(\alpha_a - \alpha_i)F^2, \tag{2}$$

where Λ is the field-free sublimation energy, I_n is the nth ionization potential of the desorbing ion, ϕ is the work function of the surface, F is the applied electric field, and α_a and α_i are the polarizability of the surface atom and desorbing ion, respectively. The second model, known as the "charge-exchange" model,[10] assumes that ionization and desorption occurs at the crossing point of the atomic and ionic potentials. According to the charge-exchange model, the activation energy is given by

$$Q(F) = \Lambda + \sum_n I_n - n\phi - \frac{(ne)^2}{4x_c} - neFx_c - \Gamma + \tfrac{1}{2}(\alpha_a - \alpha_i)F^2, \tag{3}$$

where x_c is the distance where the two curves cross and Γ is the halfwidth of the ionic level broadened by interaction with the atomic curve. Detailed discussions of the derivation of these expressions and the assumptions which underlie the two models have been reviewed extensively in the literature.[5,8,11–15] It is generally agreed that the charge-exchange model is physically more realistic than the image-force model, but it is not useful for calculations because the exact form of the atomic and ionic potentials is not known. The image-force model, on the other hand, has been quite successful in predicting the low-temperature evaporation fields for a number of metals, and has been used extensively to analyze field-evaporation data.[1] For these reasons our experimentally determined activation energies will be compared to the predictions of the image-force model. However, since our explanation for the discrepancy between theory and experiment will involve only the polarization term in Eq. (2), the suggested correction will be equally applicable to either model.

III. EXPERIMENTAL

A. Apparatus

Measurements of field-evaporation rates as a function of temperature and electric field were made with the imaging atom probe[16] shown schematically in Fig. 1. In this instrument the sample tip is spotwelded to a 5-mil (1 mil $= 10^{-3}$ in.) diameter Pt wire loop and placed in thermal contact with the cold head of a closed-cycle liquid-helium refrigerator. The tip temperature is raised from its base value of ~ 50 K by passing a dc current through the wire loop and monitored by measuring the voltage drop across the end of the loop with the two 1-mil Pt wire leads. The method used for determining the tip temperature is described below. In our experimental setup the constant-current power supply and meters for recording voltages and currents are isolated to allow the application of high voltages while the tip is being heated.

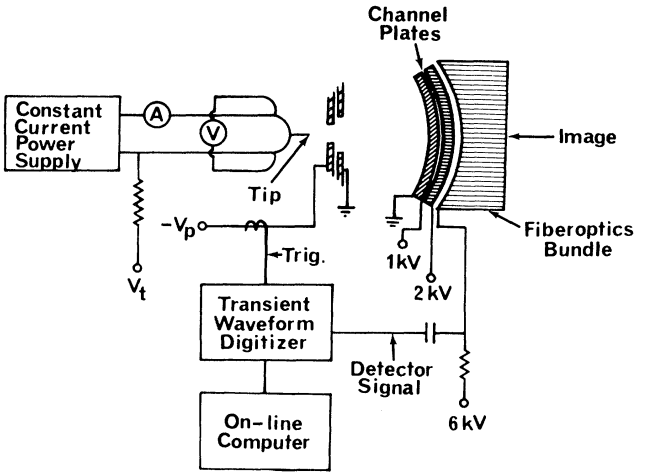

FIG. 1. Schematic drawing of the imaging atom probe used in this study.

As indicated in Fig. 1, pulsed field evaporation is initiated by applying a positive, dc bias voltage to the tip and a negative, high-voltage pulse to a counterelectrode. This procedure avoids the problems associated with applying a high-voltage pulse to the tip while it is connected to the temperature-control electronics. The field-evaporated ions are detected using the channel-plate, fluorescent-screen assembly also shown schematically in Fig. 1. This detector, which is sensitive to single-ion events, produces both an electrical pulse and an image spot for each impinging ion.[17] When two or more ions arrive at the detector simultaneously, the amplitude of the output signal is proportional to the number of ions striking the detector (see below) and multiple-ion events can be counted.[17] In our apparatus the output signal is displayed on the sweep of a fast, transient-wave form digitizer. An example of a digitizer trace taken from this study is shown in Fig. 2. The sweep is triggered by a portion of the high-voltage evaporation pulse, which is superimposed on the trace for a zero time reference. The signals corresponding to the field-evaporated ions appear as subsequent peaks in the digitizer trace separated according to their mass-to-charge ratio.[17] In Fig. 2 both W^{4+} and W^{3+} ions are observed. The change in amplitude of a given peak is used to monitor the change in evaporation rate as described below.

B. Peak height calibration

An important step in this investigation was to ascertain that the amplitude of the peaks observed in imaging

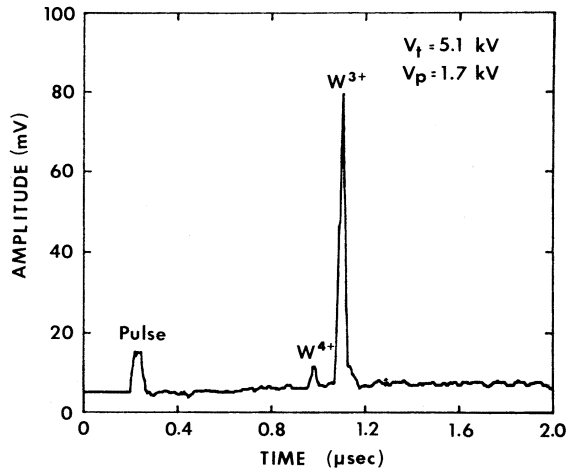

FIG. 2. Imaging atom-probe mass spectrum taken from a tungsten sample using the negative voltage pulsing described in the text.

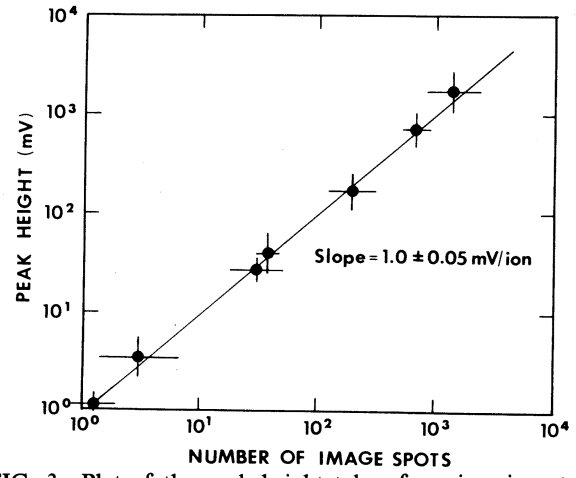

FIG. 3. Plot of the peak height taken from imaging atom-probe mass spectra vs the number of image spots taken from time-gated photographs at the same evaporation rate. The peak height is directly proportional to the number of image spots over more than 3 orders of magnitude.

atom-probe mass spectra were directly proportional to the number of ions striking the detector and to determine the proportionality constant. This was accomplished by comparing the peak amplitudes to the number of image spots on the fluorescent screen. To avoid counting random noise on the ion detector as field-evaporated ions, the channel plates were time gated for the arrival of W^{3+} ions. In the time-gating technique,[17] the second channel plate of the chevron pair is pulsed on in coincidence with the arrival of the ionic species of interest. A photograph of the screen then records image spots produced by that species only. Because the "gate-pulse" interferes with the output pulse of the detector, it is not possible to record mass spectra and time gate the channel plates simultaneously. The comparison was therefore carried out by first recording a series of five mass spectra at a given rate of field evaporation and subsequently recording five time-gated images at the same rate. The peak heights and number of image spots were then averaged to give the number of ions per mV of peak amplitude. In Fig. 3 the results of the comparison are shown. The peak heights are linear with the number of image spots over more than 3 orders of magnitude. The slope of the line yields a proportionality constant of 1.0 mV/ion. Thus we have established that the response of the channel plates is linear for a given species over a wide range of ion intensities. It should be noted, however, that the proportionality constant of 1.0 mV/ion applies only to the ions which are detected and does not take into account the efficiency of the channel plates. Without biasing the front channel plate, this efficiency is ~50% (Ref. 17) so the signal amplitude per *field-evaporated* ion is 0.5 mV/ion. This proportionality constant applies only to our specific operating conditions, and will vary depending on the species detected, the applied desorption voltages, and the gain of the particular channel plates being used.

C. Field-strength calibration

The magnitude of the electric field during the interval of the high-voltage pulse was determined by comparing the total applied voltage, $V_{dc}+V_p$, to the low-temperature dc evaporation voltage, V_0, at which the electric field strength is known. Here V_{dc} is the positive dc bias voltage applied to the tip and V_p is the amplitude of the negative high-voltage pulse applied to the counterelectrode. Normally, the pulse amplitude can be reasonably approximated by taking half of the cable charging voltage used in the pulse generator.[17] However, due to the arrangement of electrodes in our system (see Fig. 1), part of the negative voltage pulse is shunted to ground potential. To determine the amount of the resulting attenuation, a calibration was carried out comparing the amplitude of the positive voltage pulse supplied directly to the tip to the amplitude of the negative voltage pulse required to produce identical rates of field evaporation. From this procedure we determined the attenuation to be approximately 15%.

Given V_{dc} and V_p, the electric field strength F can be calculated from

$$F=\frac{V_{dc}+V_p}{V_0}F_0\,, \tag{4}$$

where V_0 is the measured low-temperature evaporation voltage and F_0 is the known low-temperature evaporation field. The low-temperature evaporated voltage, V_0 was taken as the voltage which produced a rate of evaporation of one (110) layer per 5 sec when the tip temperature was at its base value of ~50 K. The rate of evaporation was determined directly by viewing a vacuum field-desorption image. The low-temperature evaporation field was taken from a field-strength determination by Sakurai and Müller.[18] They found that the evaporation field of W at 78 K was 5.7 V/Å above the (110) plane. Since their calibration was carried out in the presence of an imaging gas, which lowers the evaporation field by several percent, the low-temperature field for our measurements (carried out in UHV), was taken to be $F_0=6.0$ V/Å.

Owing to the uncertainties in the field-strength calibration, the voltage pulse amplitude, and the variation in electric field across the sample surface, the percent error

in the absolute value of the field strengths determined from the above calibration is estimated to be 10—15%. However, the precision of the field strengths is limited only by the error in the voltage readings on the high-voltage power supplies, which is much less than 1%. Thus relative field-strength measurements are quite accurate, but absolute field strengths are subject to considerable uncertainty.

D. Temperature calibration

The measurements of field-evaporation activation energies require accurate control and monitoring of the tip temperature. In our experiments the tip was heated by passing a dc current through the platinum support loop, and the temperature was determined by measuring voltage drop across the end of the loop.[19] The current and voltage define the resistance of the end of the loop, which is related to its temperature by[20]

$$R - R_0 = \alpha R_0 (T - T_0) , \tag{5}$$

where R is the resistance at temperature T, R_0 is the resistance at temperature T_0, and α is the temperature coefficient of resistivity [$0.003\,927 C^{-1}$ for Pt (Ref. 21)]. To use Eq. (5) it is necessary to determine the resistance R_0 at a known temperature T_0. The most convenient calibration temperature is $T_0 = 300$ K when the entire system is at room temperature. As in the case of unknown temperatures, the resistance R_0 is measured by passing a current through the loop. Since even very low currents (2—20 ma) cause some heating to occur, the room-temperature resistance is determined by taking a series of current-voltage measurements and extrapolating the resistance back to zero current. Once the values of R_0 and T_0 are determined, the sample is cooled to its base value of ~ 50 K. The tip can then be heated to any temperature between its base value, and the melting point of the wire loop and its temperature can be determined by using Eq. (5).

There are two factors which affect the accuracy of the temperature determined from Eq. (5).[22] One inaccuracy arises from the fact that the platinum support loop serves as both the heating element and the thermometer. Resistive heating of the loop produces a thermal gradient between the center of the loop (where the tip is mounted) and the cryogenically cooled sapphire block (where the loop is mounted). The temperature determined by the above procedure is therefore not the tip temperature, but the average temperature across the portion of the loop between the potential leads. The difference can be as much as ~ 10 K (Ref. 22). With the use of the temperature dependence of field evaporation, it is possible to accurately determine the difference. However, since we are concerned here primarily with temperature changes, not absolute temperatures, the correction was not made. To avoid differences which would occur in changing from one tip loop to another, all measurements reported here were made on the same tip.

A second inaccuracy arises from the fact that the temperature coefficient of resistivity is not constant at low temperatures. However, the error introduced is only ~ 0.5 K when the temperature is above 200 K, and our tip temperatures seldom fell below this value. Thus we estimate the accuracy of the temperature readings to be ± 5 K and the precision $< \pm 1$ K.

E. Field-evaporation rate measurements

If N atoms on a field-emitter surface are all subjected to the same temperature, T, and electric field, F, and n of these atoms field-evaporate in a time interval, τ, then the average rate of field evaporation is given by

$$k_e(F,T) = (n/N)/\tau \tag{6}$$

(measured in $\sec^{-1}$). In our experiments surface atoms were field-evaporated by the addition of a high-voltage electrical pulse of duration 50 nsec to a dc bias voltage. The number of field-evaporated ions in each pulse was determined from the peak heights of imaging atom-probe mass signals as described above.

In order to increase the signal intensity per pulse, ions were collected from the entire imaged area of the surface. Figure 4 shows field-ion images of the emitter surface taken near the beginning and end of the experiments. These

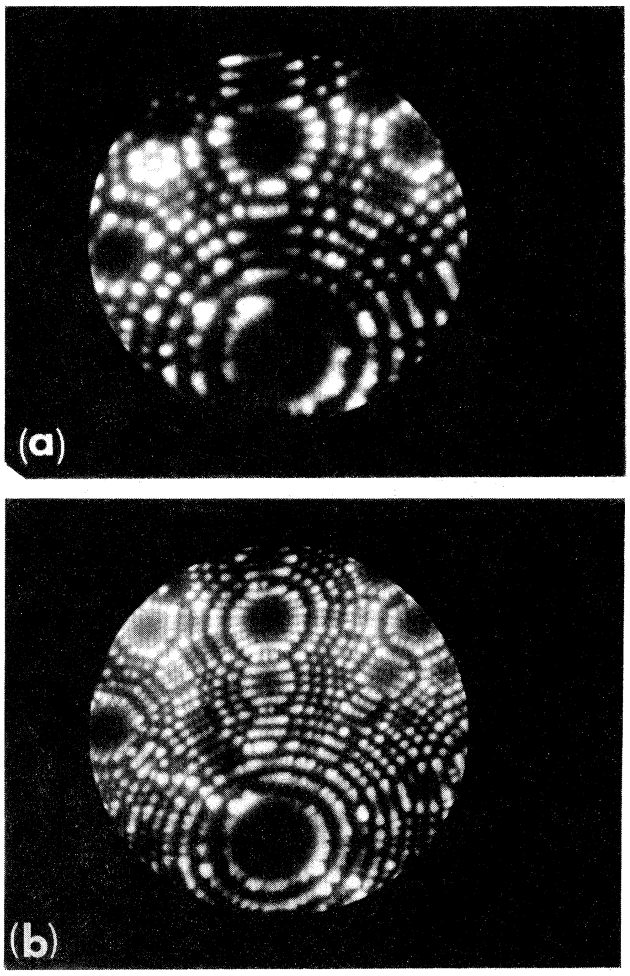

FIG. 4. Field-ion microscope images of the tungsten surface used in this study. Image (a) was recorded near the beginning of the study at $V = 3.75$ kV, and image (b) was recorded near the end of the study at $V = 5.95$ kV. Both images were recorded in He at 1.3×10^{-5} Torr.

images indicate the variation in surface sites sampled during the measurements. From direct images of field-evaporated ions (field-desorption images) at high evaporation rates, the number of surface atoms, N, in sites from which field evaporation is most likely to occur is estimated to be $N=2000$. This number obviously increases as the tip radius increases and is only a rough estimate. The error in N, however, does not affect the activation energies of field evaporation, which depend only on changes in this rate as a function of temperature.

Since ions are being collected from the entire imaged surface, we must also consider the variation in electric field from one region to another. It is assumed in Eq. (5) that all N atoms are subjected to the same electric field; whereas, in reality, the field can vary by as much as 10% over the surface. Thus the electric field at the time of desorption is not a specific value, F, but a field interval, $F+\Delta F$. However, since the majority of field evaporation is from the (110) steps (as evidenced by vacuum field-desorption images[17]) the value of ΔF is much less than the 10% variation in field strength over the surface.

The determination of absolute field-evaporation rates from Eq. (6) also requires a knowledge of the time interval, τ, over which field evaporation occurs. If the high-voltage desorption pulse were perfectly rectangular with zero rise and fall times, the time interval would be $\tau=50$ nsec. However, it is well known that high-voltage pulse seen by the tip usually has considerable structure,[17] and desorption may occur early in the pulse only. Examination of the rise times of ion signals seen in our mass spectra indicated that this was indeed the case. Allowing for the increase in rise time due to the isotopic spread of W ions, the rise times were never more than 20 nsec. Thus, instead of taking $\tau=50$ nsec, our analysis assumes $\tau=20$ nsec. Again, the error in the time interval will affect only the absolute field-evaporation rates, and not the activation energies of field evaporation.

Taking into account the above approximations, field-evaporation rates for tungsten ions were determined from Eq. (6). The measurements were made as a function of temperature for fixed values of the electric field. Once a specific dc holding voltage and pulse voltage were chosen, the temperature of the tip was increased until ion signals began to appear in the mass scans. At this point 5—10 mass scans were recorded, and the average peak heights for W^{3+} and W^{4+} signals were determined. The temperature was then increased and the same number of mass scans were recorded at each temperature setting. Depending on the field strength, 4—6 temperature settings were used to obtain an Arrhenius plot, with the maximum evaporation fluxes of the order of 1000 ions/sec. It was noted that when the sample temperature exceeded 500 K, the Arrhenius plots became nonlinear. This was most likely due to the onset of kink-site atom mobility, which changes the initial state for the field-evaporation process. For this reason, 500 K was taken as the upper limit on the temperature. This limit placed a lower limit on the field strength at ~ 4.7 V/Å. This series of rate versus temperature measurements was repeated at seven different voltage settings, and the resulting Arrhenius plots are presented in the next section.

IV. RESULTS AND DISCUSSION

A. Activation energies and Arrhenius prefactors

Plots of the log of the evaporation rate determined from Eq. (6) versus the inverse temperature corresponding to six different electric field strengths are shown in Fig. 5. The sum of the W^{3+} and W^{4+} peak heights taken from 5 to 10 individual mass spectra were averaged to obtain each data point, and the error bars reflect the standard deviation of the mean. Data were also recorded at a field strength of 4.70 V/Å, but the results are not plotted in Fig. 5 because the data points nearly overlap those recorded at 4.93 V/Å. As expected, the resulting plots are linear. From a least-squares analysis of the data, the slope and intercept of each plot were calculated, and from these values the activation energies and frequency prefactors were obtained. The results are summarized in Table I. The activation energies were found to decrease from 0.90 to 0.12 eV as the electric field was increased from 4.70 to 5.90 V/Å. The values obtained for the activation energies were roughly 1—10% of the field-free sublimation energy for tungsten (8.66 eV). The monotonic decrease in the activation energy of field evaporation as the field is increased is the expected result, since increasing the electric field should lower the potential barrier for field evaporation.

The magnitudes of the frequency prefactors listed in Table I were also found to decrease as the electric field strength was increased. This result was somewhat surprising, since it has generally been assumed that the frequency factor is independent of field.[5,8] However, changing the electric field will obviously change the shape of the potential well of the field-evaporating ion, so changes in the vibrational frequency with electric field are conceivable. As mentioned earlier, the absolute values of the frequency prefactors are dependent on the choice of N and τ and are subject to considerable uncertainty (at least an order of magnitude). The relative changes with respect to the field, however, are accurate, and the field dependence of the frequency prefactor is believed to be a real effect.

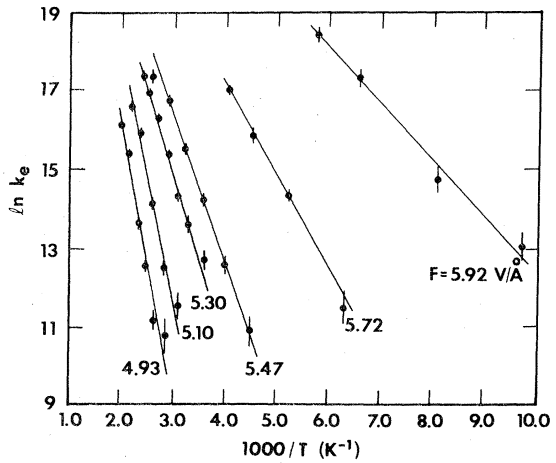

FIG. 5. Arrhenius plots for the field evaporation of tungsten. The error bars reflect the statistical deviation from the average of 5—10 mass scans.

TABLE I. Field dependences of the activation energy and frequency prefactor for field evaporation of tungsten ions.

Field (V/Å)	Q (eV)	k_0 (sec^{-1})
4.70	0.90±0.04	3×10^{16}
4.93	0.60±0.01	1×10^{13}
5.10	0.52±0.01	8×10^{12}
5.30	0.35±0.003	7×10^{11}
5.47	0.31±0.008	7×10^{11}
5.72	0.20±0.004	3×10^{11}
5.90	0.12±0.012	4×10^{11}

The rates of evaporation plotted in Fig. 5 were calculated using the total tungsten ion signal, i.e., $W^{3}+W^{4+}$. At relatively low-field strengths, no W^{4+} was detected, and the activation energies corresponded to W^{3+} ions alone. At higher-field strengths, the fraction of W^{4+} ions compared to W^{3+} became appreciable (~10% at 5.9 V/Å), and measurements of evaporation rates corresponding to each signal separately were possible. A comparison between Arrhenius plots corresponding to W^{3+} and W^{4+} is shown in Fig. 6. The field strength for the measurements was 5.92 V/Å. Within the experimental uncertainty the activation energies are equal. This result implies that the same thermally activated process is responsible for the production of both species and is consistent with the postulation that multiply charged field-evaporated ions are produced by post ionization,[7,23] i.e., ionization after evaporation. A similar result has been reported by Ernst[7] for Rh^{+} and Rh^{2+}. Since the same thermally activated process produces both W^{3+} and W^{4+}, the absolute rate of evaporation corresponds to the total ion yield, which is the reason why the rates in Fig. 5 were calculated using the sum of the two peak heights. In this study only W^{3+} and W^{4+} ions were detected, and the minimum field strength was 4.74 V/Å. This is consistent with a pulsed-laser atom-probe study of charge states as a function of field,[24] which showed that W^{2+} ions are not detected unless the field strength is below ~4.0 V/Å.

All of the above measurements were carried out with the base pressure in the vacuum system at or below 2.0×10^{-10} Torr. If the base pressure was any higher than this value, the residual gases in the system strongly influenced the rate measurements. Figure 7 shows an Arrhenius plot corresponding to data recorded at a base pressure of $\sim5\times10^{-10}$ Torr. The data points obviously do not follow a straight line. Our interpretation of the data is that contaminant gases (mostly H_2) are field-adsorbed on the surfaces at temperatures below ~200 K. The hydrogen reduces the activation energy for field evaporation (hydrogen promotion of field evaporation is a well-established effect[8]). Above ~200 K, hydrogen does not field adsorb due to its low binding energy, and the field-evaporation process proceeds as normal. The data in Fig. 7 can, therefore, be represented by two straight lines: one corresponding to hydrogen-promoted field evaporation (below 200 K) and one corresponding to normal field evaporation (above 200 K). From the slopes of the straight lines we find that the hydrogen-promotion effect reduces the activation energy from 0.26 to 0.06 eV, a considerable reduction considering that the background pressure in the system was in the mid 10^{-10} Torr range. The value of 0.26 eV at a field strength of 5.56 V/Å is clearly consistent with the activation energies taken at lower background pressures (see Table I) supporting the argument that this value corresponds to field evaporation from the contamination-free surface. The strong influence of the residual gases on the field-evaporation process at such low background pressures is an important observation, since most atom probes are operated in the low 10^{-9} Torr range. There is already evidence that the hydrogen-promotion effect can strongly influence the apparent composition of alloys determined by atom-probe analysis.[25]

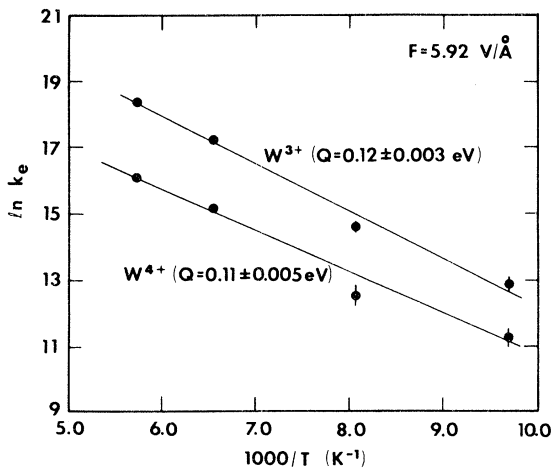

FIG. 6. Comparison of Arrhenius plots for W^{3+} and W^{4+} ions. Within the experimental uncertainty the activation energies for field evaporation are the same.

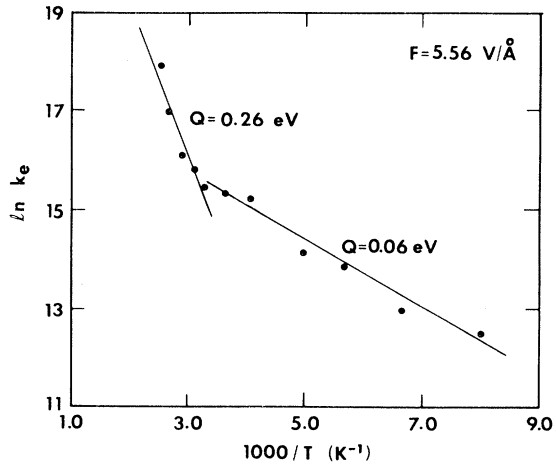

FIG. 7. Arrhenius plot for the field evaporation of tungsten in a background of $\sim5\times10^{-10}$ Torr. The residual gases have a pronounced effect on the field-evaporation process.

B. Temperature dependence of the evaporation field and field sensitivity

Measurements of the reduction in the evaporation field of W with increasing temperature have been reported previously by Nakamura and Kuroda[26] and Kellogg.[27] In the former study dc field evaporation was employed, and the temperature was varied from 21 to 300 K. In the latter study a comparison between dc and pulsed field evaporation was made, and the temperature was varied from 50 to 500 K. Allowing for the reduction in evaporation field due to the presence of helium in the former study, the two dc evaporation results were in reasonable agreement. Because the temperature dependence of the evaporation field provides additional information on the field-evaporation process and should be consistent with the appropriate theoretical models, the latter measurement was repeated in this study using the same sample tip, temperature calibration, and field calibration as used for the activation energy measurements. The results are shown in Fig. 8. As noted previously and indicated in Fig. 8, the temperature dependence of the evaporation field is strongly influenced by the rate of evaporation. When dc evaporation is used, the evaporation field decreases from 6.0 to 2.4 V/Å as the temperature is increased from 50 to 550 K. When pulsed field evaporation is employed, the decrease is from 6.0 to 4.0 V/Å over the same temperature range.

The variation in field-evaporation rate with increasing field strength at fixed temperatures was also measured in this study. Again, the measurements were carried out on the same tip with the same temperature and field-strength calibration. This type of measurement has been reported in the past for dc field evaporation by Brandon[28,29] and for pulsed field evaporation by Tsong.[5] In both previous studies the temperature was kept in the range 78–90 K. In this study, we examined the effect of changing the temperature on the field sensitivity of the evaporation rate. Figure 9 shows the results. At low temperatures ($\sim$50 K) the evaporation rate rises very rapidly with increasing field strength, but when the temperature is set at higher values, the field sensitivity is reduced. This is consistent with the above results on the temperature dependence of the evaporative field. The absolute rate of field evaporation at low temperatures is found to be in reasonable agreement with the results of Tsong,[5] i.e., $k_e = 10^6 - 10^7$ sec^{-1} at $V/V_0 = 1.05$.

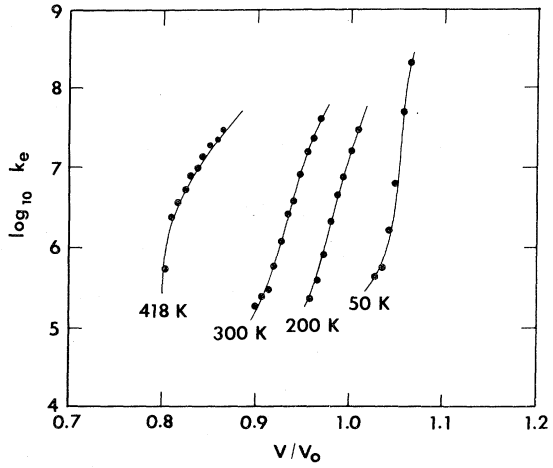

FIG. 9. Field dependence of the tungsten field-evaporation rate for four different temperatures (to convert the x axis to field strength multiply by $F_0 = 6.0$ V/Å).

V. COMPARISON WITH THEORY

The activation energies of field evaporation measured in this study (see Table I) are plotted as a function of electric field in Fig. 10. In the same figure the results of calculations based on the image-force model [i.e., Eq. (2)] are shown. The theoretical results are plotted for evaporation charge states of $n = 2$ and 3. Since the theoretical curves depend strongly on the polarization term [i.e., the choice of $\alpha = \alpha_a - \alpha_i$ in Eq. (2)] which are unknown, the curves were drawn to agree with the experimental activation en-

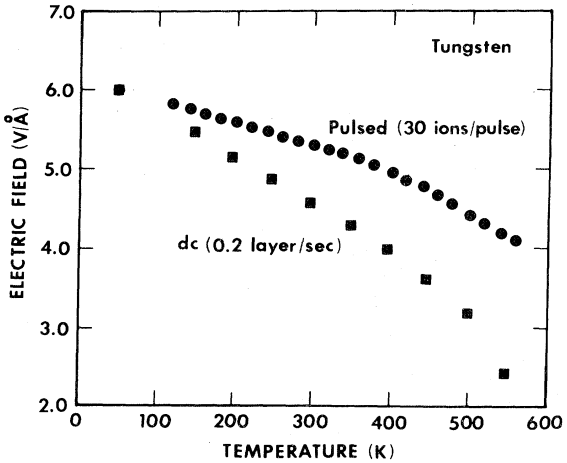

FIG. 8. Temperature dependence of the tungsten evaporation field for pulsed and dc field evaporation.

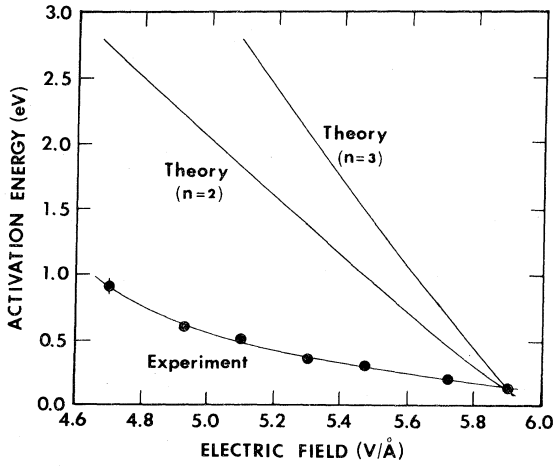

FIG. 10. Comparison between experimental and theoretical activation energies for field evaporation of W ions as a function of field strength. The polarization correction is adjusted in the theoretical calculations to force agreement between theory and experiment at 5.9 V/Å.

ergy at 5.9 V/Å. The effective polarizabilities, α, which produced this agreement were 0.48 Å^3 for $n=2$ and 2.42 Å^3 for $n=3$. As in Ernst's study of rhodium,[7] the agreement between theory and experiment is poor. In fact, there were no choices of the polarizability which produced any reasonable agreement with experiment. We are left with the conclusion that the image-force model is inappropriate for explaining the field-evaporation process.

If the classical field-evaporation model were at all realistic, the term in the expression for the activation energy which is most questionable is the polarization term, $-\frac{1}{2}\alpha F^2$. An F^2 dependence of polarization energy is appropriate for the polarization of an atom or ion in free space, but there is no reason to expect that the same dependence will hold for an atom or ion on a surface. In fact, in a high-positive electric field, a kink-site atom will most likely transfer some electronic charge to the substrate and become partially ionized, as in the case of chemisorbed atoms. Field-induced charge transfer has been discussed previously by Tsong and Kellogg,[30] who show that the amount of charge transfer in a field, F, can be approximated by

$$q(F)=e\int_{\epsilon_f-eF_{x0}}^{\epsilon_f}\rho(\epsilon)d\epsilon\ , \tag{7}$$

where e is the elementary charge, ϵ_f is the Fermi level of the surface, x_0 is the effective distance of the adatom of a kink-site atom from the surface, and $\rho(\epsilon)$ is the local density of states of the field-evaporating atom. Considering this effect, the polarization correction to the activation energy should contain an additional term $(qFx_0-q/4x_0)$ where q is given by Eq. (7). Unfortunately, calculation of $q(F)$ from Eq. (7) is very difficult. The local density of states of a kink-site atom is not known, and even if one were to approximate $\rho(\epsilon)$ by the bulk density of states, it would still be dependent on F and x_0, which makes the integral in Eq. (7) very complicated. With the use of a series of approximations, an attempt to determine $q(F)$ in the field range of interest was undertaken, and the results were in the right range to correct the activation energies [i.e., $q(F)$ values were of the order of $(0.1-0.5)e$ and increased with field]. However, the approximations involved too many adjustable parameters to make the comparison physically realistic. Therefore, the field-induced, charge-transfer effect remains only as a suggested correction to improve the image-force model and give an accurate description of the field-evaporation process. More extensive theoretical work is clearly required to establish the effect quantitatively.

The temperature dependence of the evaporation field (Fig. 8) also does not agree with recent theoretical calculations[31] based on the charge-transfer model of field evaporation. The theoretical model, which assumes a parabolic surface atom bonding well, predicts the appropriate temperature dependence of the evaporation field at low temperature (<150 K). At higher temperatures, however, the model fails, probably because the parabolic approximation breaks down at temperatures above 150 K. Corrections involving polarization effects may also be important in this calculation.

VI. SUMMARY

In this paper we have shown that activation energies of field evaporation can be measured directly from the change in amplitude of imaging atom-probe mass signals with respect to temperature. The procedure was applied to field evaporation of tungsten, and activation energies were determined at seven different field strengths ranging from 4.70 to 5.90 V/Å. The qualitative dependence of the activation energy on electric field was found to be correct, i.e., the activation energy increased with decreasing field strength, but the quantitative values did not agree with calculations based on the image-force model of field evaporation. To improve the agreement, a polarization correction taking into account field-induced, charge-transfer effects was suggested. An unexpected result of this study was the observation that the frequency prefactor in the Arrhenius rate equation is also a field-dependent quantity. Activation energies for field evaporation of W^{3+} and W^{4+} were found to be the same supporting the concept of post ionization for the production of multiply charged ions. It was also noted in this study that very low levels of residual gases in the vacuum chamber can have an overwhelming influence on the field-evaporation process, and this influence can have important implications for quantitative atom-probe measurements.

Although we have developed no satisfactory model to explain the field dependence of the activation energy for field evaporation, the systematic data reported in this study should provide a quantitative test of models developed in the future. With the development of such models (which may require a full quantum-mechanical treatment of the field-evaporation process), the ultimate goal of using evaporation field strengths to obtain site-specific binding energies may then be attained.

ACKNOWLEDGMENTS

This work was performed at Sandia National Laboratories supported by the U. S. Department of Energy under Contract No. DE-AC04-76DP00789.

[1]See, for example, E. W. Müller and T. T. Tsong, *Field Ion Microscopy, Principles and Applications* (Elsevier, New York, 1969).

[2]G. Ehrlich and C. F. Kirk, J. Chem. Phys. 48, 1465 (1968).

[3]E. W. Plummer and T. N. Rhodin, J. Chem. Phys. 49, 3479 (1968).

[4]E. W. Müller, in *Molecular Processes on Solid Surfaces,* edited by E. Drauglis, R. D. Gretz, and R. I. Jaffe (McGraw-Hill, New York, 1968), p. 401.

[5]T. T. Tsong, J. Chem. Phys. 54, 4205 (1971).

[6]M. Vesely and G. Ehrlich, Surf. Sci. 34, 547 (1973).

[7]N. Ernst, Surf. Sci. 87, 469 (1979).

[8]See, for example, E. W. Müller and T. T. Tsong, *Progress in Surface Science,* edited by S. G. Davison (Pergamon, New

York, 1973), Vol. 4, Part 1.
[9]E. W. Müller, Phys. Rev. 102, 618 (1956).
[10]R. Gomer, J. Chem. Phys. 31, 341 (1959).
[11]D. G. Brandon, Surf. Sci. 3, 1 (1964).
[12]D. McKinstry, Surf. Sci. 29, 37 (1972).
[13]R. G. Forbes, Surf. Sci. 70, 239 (1978).
[14]G. L. Kellogg and T. T. Tsong, Surf. Sci. 62, 343 (1977).
[15]R. G. Forbes, Surf. Sci. 102, 255 (1981).
[16]J. A. Panitz, Rev. Sci. Instrum. 44, 1043 (1973).
[17]J. A. Panitz, *Progress in Surface Science,* edited by S. G. Davison (Pergamon, New York, 1973), Vol. 8, Part 6.
[18]T. Sakurai and E. W. Müller, J. Appl. Phys. 48, 2618 (1977).
[19]See, for example, G. Ayrault and G. Ehrlich, J. Chem. Phys. 60, 281 (1974).
[20]H. F. Stimson, in *Precision Measurement and Calibration: Temperature,* Natl. Bur. Stand. (U.S.) Spec. Publ. No. 300, edited by J. F. Swindells (U. S. GPO, Washington, D.C., 1968), Vol. 2, p. 121.
[21]*Materials Handbook,* edited by T. Lyman (American Society for Metals, Metals Park, Ohio, 1961), Vol. 1, p. 798.
[22]See, for example, P. L. Cowan, Ph.D. thesis, Pennsylvania State University, 1977 (unpublished).
[23]R. Haydock and D. R. Kingham, Phys. Rev. Lett. 44, 1520 (1980).
[24]G. L. Kellogg, Phys. Rev. B 24, 1848 (1981).
[25]R. Herschitz and D. N. Seidman, Surf. Sci. 30, 63 (1983).
[26]S. Nakamura and T. Kuroda, Surf. Sci. 17, 346 (1969).
[27]G. L. Kellogg, J. Appl. Phys. 52, 5320 (1981).
[28]D. G. Brandon, Br. J. Appl. Phys. 16, 683 (1965).
[29]D. G. Brandon, Philos. Mag. 14, 803 (1966).
[30]T. T. Tsong and G. L. Kellogg, Phys. Rev. B 12, 1343 (1975).
[31]K. Chibane and R. G. Forbes, Surf. Sci. 122, 191 (1982).

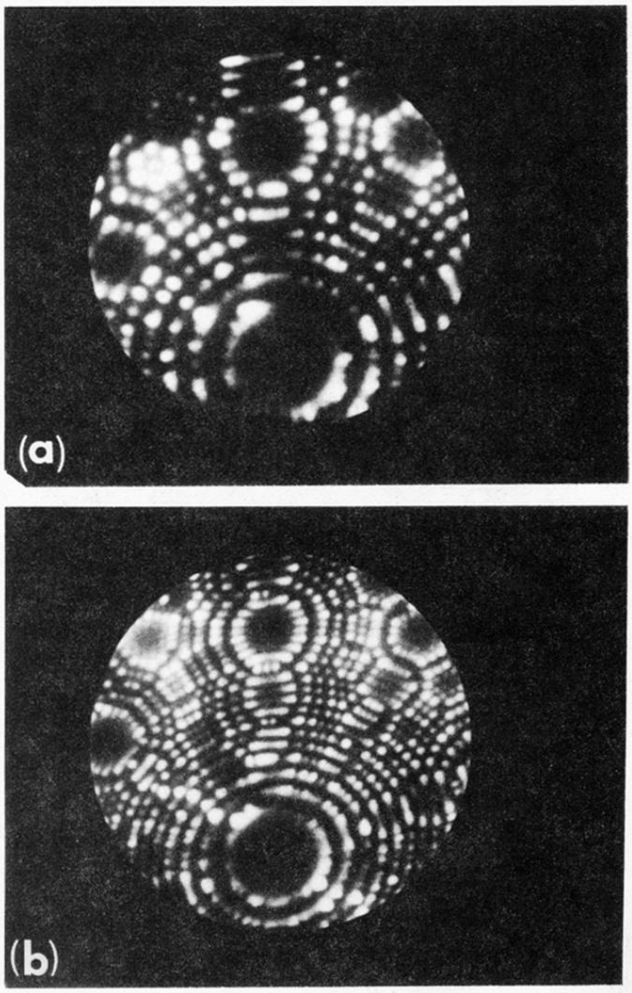

FIG. 4. Field-ion microscope images of the tungsten surface used in this study. Image (a) was recorded near the beginning of the study at $V=3.75$ kV, and image (b) was recorded near the end of the study at $V=5.95$ kV. Both images were recorded in He at 1.3×10^{-5} Torr.